existence in solutions contacting the potassium mirror, since their ESR spectra are not observed. This statement refers to $\mathbf{1a}^{\bullet-}$ (a valence isomer of $\mathbf{1}^{\bullet-}$) as well as to $\mathbf{8}^{\bullet-}$ and $\mathbf{4}$-H(1)$^{\bullet-}$ in pathway A or to $\mathbf{9}^{\bullet-}$ and $\mathbf{5}$-H(4)$^{\bullet-}$ in pathway B. In particular, $\mathbf{5}$-H(4)$^{\bullet-}$ should readily convert into $\mathbf{5}^{\bullet 2-}$, as do the isomeric radical anions $\mathbf{5}$-H(1)$^{\bullet-}$, $\mathbf{5}$-H(2)$^{\bullet-}$, and $\mathbf{5}$-H(3a)$^{\bullet-}$ which undoubtedly are the primary reduction products of the reaction starting from a mixture of corresponding neutral bicyclo[6.3.0]undecatetraenes and yielding $\mathbf{5}^{\bullet 2-}$ as a single final product (see Results). It is noteworthy that a thermal rearrangement of the neutral **1** into a variety of products can be accounted for by a pathway involving the intermediates **1a**, **9**, and **5**-H(4) (a known compound[35]), whereas an alternative route via **1a**, **8**, and **4**-H(1) has to be disregarded.[36] This result may be combined with the present finding that addition of HMPT to DME or MTHF changes the course of reaction from pathway A to B. Since solvation by HMPT weakens the association between a hydrocarbon anion and its alkali metal counterion, such a change is presumably due to a loosening of ion pairing. The available evidence thus enables one to suggest that the rearrangement of **1** to the π-system of **5** is preferred for a neutral compound or a nonassociated radical anion, whereas pairing of $\mathbf{1}^{\bullet-}$ and/or $\mathbf{1a}^{\bullet-}$ with the counterion K^+ favors the rearrangement to the π-system of **4**.

Concluding Remark. The present studies on the radical anion of homoazulene (**1**) stress the *important role of homoconjugation* in determining the electronic structure of the compound **1**. In accord with the prediction of the simple perturbation treatment applied here to the degenerate lowest antibonding MO's of the 10-membered perimeter, the LUMO of **1** is *symmetric* with respect to the mirror plane passing through two opposite π-centers, and it thus correlates with the corresponding MO of azulene (**3**). When an analogous treatment is used for the degenerate highest bonding perimeter MO's, an energy sequence closely resembling that depicted in Figure 4 for **1** is obtained. This means that again, due to homoconjugation, the symmetric MO should be stabilized relative to its antisymmetric counterpart. It is, therefore, an *antisymmetric* MO which is expected to become the HOMO of **1** and thus to correlate with the corresponding MO of **3**.[9] The similar nodal properties of both frontier orbitals in **1** and **3** provide a theoretical basis for rationalizing the electronic features common to the two compounds such as adherence of the long-wave absorption band to Plattner's rules. These common features fully justify the name of homoazulene given to the novel bridged [10]annulene **1**.

(34) Haddon, R. C.; Scott, L. T. *Pure Appl. Chem.* **1986**, *58*, 137.
(35) Scott, L. T.; Brunsvold, W. R. *J. Am. Chem. Soc.* **1978**, *100*, 6535.
(36) Scott, L. T.; Erden, I. *J. Am. Chem. Soc.* **1982**, *104*, 1147.

Experimental Section

Materials. Homoazulene (1). The synthesis of **1** has been described previously.[2b,4]

2-Deuteriohomoazulene (2-D-1). Deuterium was introduced into the 2-position of homoazulene at an intermediate stage in the synthesis. Thus, 180 mg (1.12 mmol) of tricyclo[5.3.1.0]undeca-3,5-dien-8-one[4] in 4 mL of tetrahydrofuran (THF) was stirred at room temperature for 15 h with 1.5 mL of 0.1 M NaOD in D_2O. After removal of THF under reduced pressure, the remaining mixture was extracted with ether. This solution was dried over magnesium sulfate, and the ether was removed under reduced pressure yielding 175 mg (96% recovery) of a nearly colorless oil. Analysis by NMR indicated >90% exchange at C(9). This material was carried on to 2-D-**1** by the procedure used previously.[4]

9-*exo*-Deuteriohomoazulene (9-exo-D-1). Under a nitrogen atmosphere, 106 mg (0.745 mmol) of homoazulene (**1**) in 2 mL of dry THF was added rapidly via syringe with stirring to a fivefold excess of lithium diisopropylamide (3.73 mmol) in 8 mL of dry THF at −78 °C. The resulting dark red solution was stirred for 3.5 min at −78 °C, and then 2.5 mL of D_2O (99.9%) was added all at once. The yellow-orange solution thus obtained was allowed to warm to room temperature. Concentration under reduced pressure at this temperature gave an orange solution which was extracted with 25 mL of *n*-pentane. The pentane layer was washed with 2 × 30 mL of saturated aqueous sodium chloride, dried over magnesium sulfate, and concentrated under reduced pressure at room temperature to yield an orange oil. Preparative layer chromatography on alumina with pentane as the eluant gave 24 mg (23%) of 9-exo-D-**1**. Analysis by NMR showed >90% incorporation of deuterium at the 9-exo position. The sterochemistry of the product follows from the finding that the long-range W-coupling (1.6 Hz) between the second hydrogen (9-endo) of the CH_2-bridging group and the hydrogens in the 1- and 3-positions has been preserved.

Bicyclo[6.3.0]undecapentaenes 5-H(1), 5-H(2), and 5-H(3a). A mixture of these three isomers, with **5**-H(1) as the major product, was obtained by irradiation of diazocyclopentadiene in benzene, according to a procedure described in the literature.[37]

Preparation of the Radical Anions. Because of instability of the neat homoazulene (bright orange oil at room temperature),[4] samples of **1**, 2-D-**1**, and 9-exo-D-**1**, synthesized in the Reno laboratory, had to be transferred to Basel as diluted solutions in pentane. In the Basel laboratory, pentane was removed under reduced pressure, and it was replaced by a solvent appropriate for the conversion of the neutral compound into its radical anion.

Instrumental. The equipment for the cyclic voltammetry included a potentiostat/galvanostat Model 173 and universal programmer 175, both of Princeton Applied Research (PAR). The spectral apparatus consisted of a Varian-ESR-E9 spectrometer with an attached Varian-ENDOR-1700 system.

Acknowledgment. This work was supported by the National Science Foundations of Switzerland and U.S.A.

(37) Schönleber, D. *Chem. Ber.* **1969**, *102*, 1789.

Double Nitrogen Inversion in Sesquibicyclic Hydrazines and Their Cation Radicals

Stephen F. Nelsen,* Timothy B. Frigo, Yaesil Kim, and James A. Thompson-Colón

Contribution from the S. M. McElvain Laboratories of Organic Chemistry, Department of Chemistry, University of Wisconsin, Madison, Wisconsin 53706. *Received May 20, 1986*

Abstract: The barrier to double nitrogen inversion in **4** (measured by observing the rate of bridgehead equilibration in $\mathbf{4}$-d_6 by ^{1}H NMR) is 27.0 kcal/mol at 80 °C, substantially higher than the 10.3 kcal/mol at −55 °C observed for **2** (by ^{13}C DNMR). The barrier to double nitrogen inversion in $\mathbf{4}^{\bullet+}$ (determined by dynamic ESR measurements on $\mathbf{4}$-$d_{12}{}^{\bullet+}$) is 4.6 kcal/mol at −85 °C. The effects of ring homologation on the amount of bend at nitrogen in sesquibicyclic hydrazines and their cation radicals as indicated by conformational and spectral measurements is discussed, and it is shown that AM1 calculations are able to predict the observed behavior rather well.

1,2-Dialkyl-1,2,3,6-tetrahydropyridazines, A, readily undergo thermal retro-Diels–Alder cleavage to dienes and azo compounds[1] (reaction 1). Conditions which allow the reverse reaction, Diels–Alder synthesis of A (Reaction 2), have only recently been

0002-7863/86/1508-7926$01.50/0

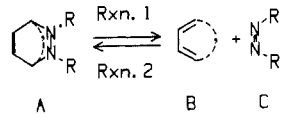

A B C

reported.[2] Despite the fact that reaction 2 replaces two π bonds by two σ bonds (which is usually distinctly exothermic), reaction 2 has been shown to be endothermic for some cyclic dienes B adding to bicyclic azo compounds C, which makes the reaction as written thermodynamically impossible to achieve in these cases. Fortunately, because azo compounds are far less basic than hydrazines, the Diels–Alder addition becomes exothermic for the protonated azo compounds. This allows efficient preparation of the thermally unstable adduct **1** and its thermally stable but very easily oxidized hydrogenation product **2**, and their analogues **3** and **4** were prepared similarly.[2] These hydrazines are of special

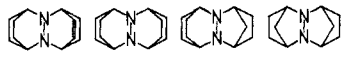

1 2 3 4

interest to us because their *N,N'*-bis-bicyclic structures force the hydrazine unit to assume its electronically least stable configuration, with the lone pair, lone pair dihedral angle θ near 0°. The bicyclic alkyl groups hold the C_α–H bonds near the nodal plane of the π rich lone pair orbitals, imparting substantial Bredt's rule kinetic protection on the oxidized compounds, allowing isolation and X-ray crystallographic structure determination of both $\mathbf{1}^{\bullet+}$ and $\mathbf{2}^{\bullet+}$.[3] The nitrogens of a neutral hydrazine in a $\theta = 0°$ conformation would prefer to be more pyramidal than tetrahedral (the average of the bond angles at nitrogen, $\alpha(av) < 109.5$), to decrease the unfavorable electronic interaction between the lone pair electrons,[4] but such pyramidalization is resisted by the syn two carbon bridges, which require **1** and **2** to have somewhat flattened nitrogen atoms. We used the dihedral angle between the two CNNC units, ϕ, in previous discussions,[3] but for considering the proton splitting constants, the direction of bending from planarity at nitrogen is important, making it desirable to use the complement of ϕ, which we will call Ψ, in this work. We

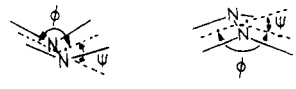

will also employ $\alpha(av)$, which is nearly linear with lone pair hybridization all the way from 109.5° to 120° in considering how deformed from planarity nitrogen atoms are. Crystalline **2** has $\Psi = 47.8°$, and $\alpha(av) = 112.0°$, corresponding to 24% of the change between tetrahedral and planar nitrogens.[3] There is also some torsion in the bicyclic rings; its CN,NC dihedral angle is 15°, which relieves steric interaction between the syn CH_2CH_2 bridges. **1** has 0° CN,NC dihedral angles, as expected because its double bond resists torsion of the bicyclic rings. The cation radical $\mathbf{1}^{\bullet+}$ has flatter nitrogens than the neutral form, $\Psi = 27.4°$ and $\alpha(av) = 117.7°$, corresponding to a bending 22% of the way from planar to tetrahedral at nitrogen. The saturated compound **2** is the most easily oxidized hydrazine known, its formal potential for first electron removal, $E°'$, being −0.53 V vs. the saturated calomel electrode.[5] Converting one and two of the four two-carbon bridges of **2** to one-carbon bridges, giving **3** and **4**, has a substantial effect on the thermodynamics for electron removal from these systems,[2b] $E°'$ values of −0.26 and +0.01 being observed, so **3** is 6.2 kcal/mol and **4** is 12.5 kcal/mol harder to oxidize than **2**. We found the magnitude of these effects for what appear to be rather small structural changes intriguingly large, and in this paper, we consider the sizes of the thermodynamic and spectral changes which accompany the ring contractions between **2** and **4**.

Results and Discussion

Double Nitrogen Inversion in Neutral 2–4. Flattening at nitrogen accompanies electron removal in amino nitrogen (R_2N–X) compounds. Because the transition state for nitrogen inversion is flat at nitrogen, alkyl group structural changes which lower the nitrogen inversion barrier rather generally make oxidation easier in cases where X is cylindrically symmetric.[6] The N–N dihedral angle does not change much upon electron removal from **2–4**, and we expected that the double nitrogen inversion barriers would be quite different for these compounds because of the large difference in their $E°'$ values.

The ^{13}C NMR spectrum of **2** consists of the expected CH_2 and CH signals at room temperature,[2] but the CH_2 signal broadens as the temperature is lowered and eventually reappears as two signals of equal intensity, which are sharp and occur at δ 28.5 and 22.9 at −89 °C in CD_2Cl_2. Double nitrogen inversion interconverts the two types of CH_2 carbon atoms, as indicated by the circles and squares on the structures below. The coalescence

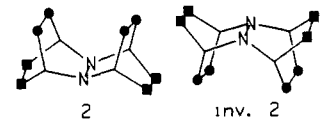

2 inv. 2

temperature is about −51 °C at 25.16 MHz, corresponding to $\Delta G^\ddagger$ for double nitrogen inversion of 10.4 kcal/mol.

The ^1H NMR spectrum of **4** at room temperature shows bridgehead hydrogens at δ 3.37 and 3.31, and its ^{13}C NMR spectrum has six carbon signals,[2b] showing that double nitrogen inversion is slow on the NMR time scale at room temperature. The bridgehead hydrogen signals do not broaden up to 130 °C in dimethyl-d_6 sulfoxide, which is only consistent with a barrier of over 20 kcal/mol for double nitrogen inversion, so the process was clearly too slow to be studied by dynamic NMR. We therefore prepared **4**-d_6 starting with the labeled diazabicycloheptene **5**-d_6, which should initially give only the endo bridgehead hydrogen isomer **n-4**-d_6 as proved to be the case, since we only observed the δ 3.37 peak by ^1H NMR. The rate of double nitrogen inversion could then be determined by observing the rate at which **n-4**-d_6 was converted to the equilibrium 1:1 mixture of **x-4**-d_6 and

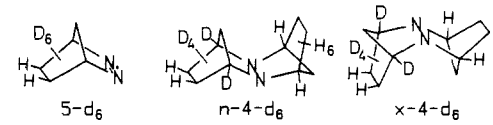

5-d_6 n-4-d_6 x-4-d_6

n-4-d_6. The rate constant for double nitrogen inversion was measured by 270 MHz ^1H NMR integration of the bridgehead hydrogen signals relative to internal *tert*-butylbenzene, giving rate constants of 2.94×10^{-5} s^{-1} at 66.0 °C in acetonitrile-d_6 and 1.98×10^{-4} and 4.62×10^{-4} s^{-1} at 81.9 and 91.9 °C in Me_2SO-d_6, respectively. These values correspond to $\Delta G^\ddagger$ values of 27.01, 26.96, and 27.13 kcal/mol, respectively, and are consistent with a very small value for $\Delta S^\ddagger$, as expected from the rigid structure of **4**.

The inversion barrier of **4** is notably high for a tetraalkylhydrazine, as can be seen from Table I and the visual display of these data in Figure 1. **4** is almost as slow to invert as the diaziridine **6**, which has a smaller CNN angle, and **4** has a 5.5 kcal/mol higher barrier than di-*tert*-butyldiazetidine **7**, in which the inversion barrier has been increased by about 4.7 kcal/mol over that of dimethyldiazetidine **8** by the necessity of forcing bulky *tert*-butyl groups past each other. Most hydrazines undergo consecutive single nitrogen inversion,[7] since it avoids flattening

(1) Nelsen, S. F. *J. Am. Chem. Soc.* **1974**, *96*, 5669.
(2) (a) Nelsen, S. F.; Blackstock, S. C.; Frigo, T. B. *J. Am. Chem. Soc.* **1984**, *106*, 3366. (b) Nelsen, S. F.; Blackstock, S. C.; Frigo, T. B. *Tetrahedron* **1986**, *42*, 1769.
(3) Nelsen, S. F; Blackstock, S. C.; Haller, K. J. *Tetrahedron*, in press.
(4) (a) Nelsen, S. F. *Acc. Chem. Res.* **1981**, *14*, 131. (b) Nelsen, S. F. *Molecular Structures and Energetics*, Liebman, J. F., Greenberg, A., Eds.; VCH Publishers, Inc.: Deerfield Beach, FL, 1986; Vol. 3, Chapter 1, p 1–86.
(5) Conditions: room temperature in CH_3CN containing 0.1 M tetrabutylammonium perchlorate as supporting electrolyte.
(6) Nelsen, S. F.; Cunkle, G. T.; Gannett, P. M.; Ippoliti, J. T.; Qualy, R. J. *J. Am. Chem. Soc.* **1983**, *105*, 3119.

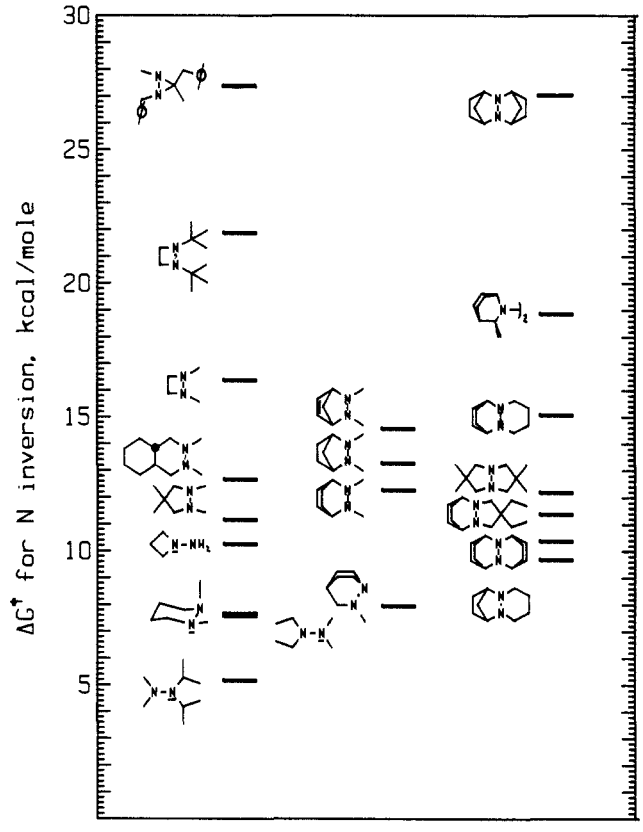

Figure 1. Double nitrogen inversion barriers for selected tetraalkylhydrazines.

two nitrogens at once, but **4** is structurally incapable of inverting just one nitrogen at a time because the small CN,NC angles required by its bicyclo[2.2.1]heptyl rings make the trans fused exo,endo isomer unobtainable. The only other hydrazine previously suggested to undergo simultaneous double nitrogen inversion is **19**. Although the nitrogens of **19** must be flattened by the ring substitution, it shows a double nitrogen inversion barrier of 18.8 kcal/mol, and its steric crowding was argued to preclude inversion at one nitrogen without at least starting to invert the other one. The large effect of N–N rotational angle on the barrier for nitrogen inversion in hydrazines, which is responsible for much of the considerable range for barriers in acyclic and six-membered ring hydrazines in the first two columns of Figure 1, has been previously discussed.[4] The subtlety of interpreting inversion barriers for hydrazines is illustrated by considering the changes in barriers observed comparing a compound having an *N,N'*-diazabicyclo[2.2.1]heptane ring to its bicyclo[2.2.2]octane ring analogue. As Anderson and Lehn showed,[8] bicycloheptane **16** has a 1.0 kcal/mol higher barrier than bicyclooctane **17**, which is reasonable, because closing a CNN angle will raise the nitrogen inversion barrier. However, for the tricyclic compounds **23** and **20**, the same structural change of closing the CNN angle by what is likely to be a similar amount causes the double nitrogen inversion barrier to decrease by 5.4 kcal/mol. As has been pointed out,[9] closing the hexahydropyridazine ring makes **23** flatten at nitrogen much more than **20**. Both compounds are trans-fused at the hydrazine unit, and bicyclic ring torsion can be much greater in the bicyclooctane **20** than in the bicycloheptane **23**. Going from the tricyclic systems **23** and **20** to the tetracyclic systems **4** and **2** reverses the barrier order again. The sesquibicycloheptane **4** has a double nitrogen inversion barrier a remarkable 16.7 kcal/mol higher than does sesquibicyclooctane **2**, and both are cis-fused at the hydrazine unit. **2** is a little harder to invert than less sterically hindered compounds which clearly invert one nitrogen at a time, and one possibility seemed to us to be that the bicyclooctane units of **2** can twist enough to make the trans-fused form of **2** an intermediate, so that its nitrogens invert one at a time. The great steric hindrance of **2**, which flattens its nitrogens substantially compared to less α-branched compounds with six-membered rings, however, makes it difficult to tell whether this is actually the case.

We would be very interested in the double nitrogen inversion barrier for the case intermediate between **2** and **4**, compound **3**, but we have been frustrated in our attempts to measure it. **3** exists exclusively as the exo isomer, as shown by its ^{13}C NMR,[2b] and

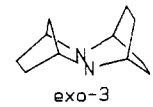

exo-3

no *endo*-**3** has been detected in equilibrium with it at any tem-

Table I. Nitrogen Inversion Barriers for Selected Tetraalkylhydrazines

structure	no.	$\Delta G^{\ddagger}$	temp, °C	ref
	6	27.3	+70	*a*
	7	21.8	+155	*b*
	8	16.3	+55	*b*
	9	12.6	+2	*c*
	10	11.1	−45	*d*
	11	10.2	−65	*e*
	12	7.6	−100	*c*
	13	7.5	−112	*f*
	14	5.1	−160	*f*
	15	14.5	+15	*g*
	16	13.2	+19	*g*
	17	12.2	−7	*h*
	18	7.9	−13	*h*
	4	27.0	+80	*k*
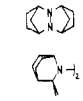	19	18.8	+63	*i*
	20	15.0	+22	*j*
	21	12.1	−29	*k*
	22	11.3	−25	*h*
	2	10.3	−55	*k*
	23	9.6	−89	*j*

[a] Mannschreck, A.; Seitz, W. *Angew. Chem.* **1969**, *81*, 224. [b] Hall, H. J.; Bigard W. S. *J. Org. Chem.* **1978**, *43*, 2785. [c] Nelsen, S. F.; Weisman, G. R. *J. Am. Chem. Soc.* **1976**, *98*, 3281. [d] Lehn, J. M.; Wagner, J. *Tetrahedron* **1970**, *26*, 4227. [e] Lehn, J. M. *Fortschr. Chem. Forsch.* **1973**, *15*, 311. [f] Lunazzi, L.; Maccantelli, D. *Tetrahedron* **1985**, *41*, 1991. [g] Anderson, J. E.; Lehn, J. M. *J. Am. Chem. Soc.* **1967**, *89*, 81. [h] Nelsen, S. F.; Weisman, G. R. *J. Am. Chem. Soc.* **1976**, *98*, 1842. [i] Nelsen, S. F.; Gannett, P. M. *J. Am. Chem. Soc.* **1982**, *104*, 5292. [j] Nelsen, S. F.; Hollinsed, W. C.; Grezzo, L. A.; Parmelee, W. P. *J. Am. Chem. Soc.* **1979**, *101*, 7347. [k] Kintzinger, J. P.; Lehn, J. M.; Wagner, J. *J. Chem. Soc., Chem. Commun.* **1967**, 206. [l] This work.

(7) See Table I, footnotes *e* and *g* for discussion of this point.
(8) Table I, footnote *e*.
(9) Table I, footnote *j*.

Table II. ESR Splitting Constants for Some Hydrazine Cation Radicals

compd	solvent	temp, °C	a(2N), G	H splittings (No. of H), G
1$^{\bullet+}$	CH_3CN	24	19.2	5.4 (4)
27$^{\bullet+}$	CH_2Cl_2	24	14.7	3.70 (2), 2.46 (2), 12.46 (6, 2 Me)
17$^{\bullet+}$	CH_3CN	24	13.6	2.46 (4, H_{exo}), 0.60 (4, H_{endo}) 13.0 (6, 2 Me)
15$^{\bullet+}$	CH_3CN	24	18.81	3.74 (2, H.v), 2.14 (1) 12.77 (6, 2 Me)
16$^{\bullet+}$	CH_3CN	24	16.0	4.8 (2, H_{exo}), 1.7 (1), 0.8 (1), 13.6 (6, 2 Me)
2$^{\bullet+}$	CH_3CN	24	15.24	2.87 (8, H_{exo}), 0.58 (8, H_{endo})
28$^{\bullet+}$	CH_2Cl_2	−80	17.2	(at least 4 H near 3.0 G)
3$^{\bullet+}$	CH_2Cl_2	−75	16.1	(at least 4 H near 5.0 G)
4$^{\bullet+}$	*n*-PrCN	+23	20.8	4.2 (4)

perature. **3** was prepared by hydrogenation of the adduct of **5H**$^+$ with cyclohexadiene, and only attack of cyclopentadiene from the less hindered, exo face of **5H**$^+$ to produce the "Alder endo rule" product **24H**$^+$ was detected.[2] We expected **25H**$^+$ to produce

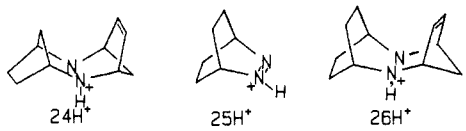

26H$^+$, which would be easily converted to *endo*-**3H**$^+$. We were dismayed to discover that several attempts to carry out this reaction failed completely and appeared to lead only to dicyclopentadiene and polymers. We shall return to the question of why the reaction failed below.

Pyramidalization at Nitrogen in Cation Radicals of 1–4. Most of the detailed structural information available from spectroscopy on cation radicals has come from ESR spectroscopy, and we will discuss the ESR spectra of these compounds first. The ESR spectrum of **1**$^+$ has g = 2.0038, but it is not particularly well resolved, as would be expected from the several types of proton splittings present (see Table II). The only proton splitting we resolved was a four hydrogen splitting of 5.4 G, which must correspond to two pairs of hydrogens with accidentally equivalent splittings. We presume that this species exists predominately as *exo*-**1**$^+$, with the saturated bicyclic ring predominantly syn to the unsaturation (as it is in the crystal[3]) for steric reasons, and attribute the observed splittings on the vinyl hydrogens and one pair of exo hydrogens in a CH_2CH_2 bridge. The data quoted in Table II for the cations of the monobicyclic analogues **27** and **15–17** show that observably large splittings would occur for both types of hydro-

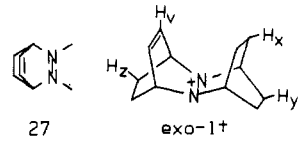

27 exo-1$^+$

gens,[10] and because we would have to expect very similar splittings for the geometrically similar Hy and Hz hydrogens of **1**$^{\bullet+}$, we must attribute the observed saturated bridge 2 H splitting to Hx, which is in W-plan to the formally spin-bearing lone-pair orbitals at nitrogen.

The more symmetrical **2**$^{\bullet+}$ showed g = 2.0036, and a better resolved spectrum, which was well simulated with the splittings given in Table II and a line width of 0.2 G. The bridgehead 4 H splitting was not observed and must be smaller than 0.2 G. This needs explaining, because the nitrogens of **2**$^{\bullet+}$ must be slightly pyramidal in solution, as they are in the crystal. Raising the temperature decreases a(2N), which is only consistent with a pyramidal nitrogen equilibrium structure.[10] In butyronitrile, the nitrogen splittings observed were 15.12_5 (+22 °C), 15.28_8 (−35 °C), 15.36_3 (−60 °C), and 15.52_5 (−85 °C), corresponding to a temperature coefficient of −3.7 mG/deg. The $B\cos^2\theta$ relationship between β splittings and the H_β–C,N–lone pair dihedral angle, using the B value of about 25.7 obtained from N–CH_3 substituted compounds,[11] gives bridgehead splittings estimated from the heavy atom geometry of crystalline **2**$^{\bullet+}$,[2b] which average to 1.0 G, which is at least five times the unobserved experimental value. The much smaller observed value may well not indicate more flattening at nitrogen than found in the crystal but instead a cancelling γ contribution to the observed splitting. Bauld and co-workers[12] have emphasized the importance of 1,3 overlap in contributions to ESR splitting constants, and the nitrogen γ to the bridgehead hydrogen has opposite spin to that which is β, so the β and γ contributions to the splitting would be expected to be of opposite sign. We suggest that they must nearly cancel for **2**$^{\bullet+}$.

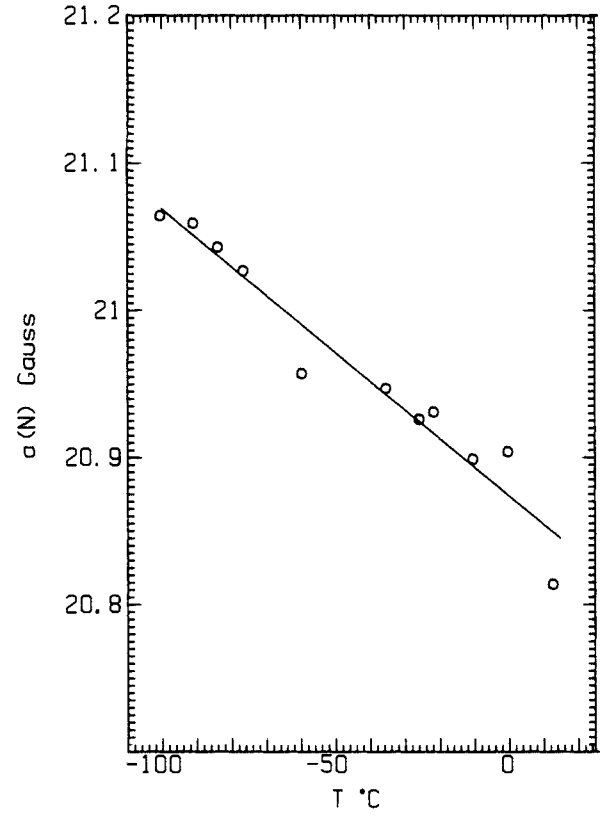

Figure 2. Temperature dependence of a(N) for **4**$^{\bullet+}$-d_{12}.

Both **3**$^{\bullet+}$ and its unsaturated precursor **28**$^{\bullet+}$ gave complex ESR spectra from which we were only able to reliably extract the

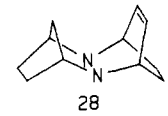

28

nitrogen splitting. Both cation radicals also show splittings in the range 3–5 G for at least four hydrogens, but the spectra were too complex and ill-resolved for us to reliably determine these splittings; we would expect three different splittings in this range for each compound, from the results obtained for **2**$^{\bullet+}$ and **4**$^{\bullet+}$. The nitrogen splitting constant for **4**$^{\bullet+}$ shows that its average amount of bend at nitrogen is significantly greater than for the other compounds of Table II, as might be expected from its more restricted CNN angles. The nitrogen splitting of **4**$^{\bullet+}$ was also found to decrease as the temperature is increased, as shown in Figure 2 (which uses data from the d_{12} compound). The least-squares line shown corresponds to a temperature coefficient of −1.8 mG/deg, only half that found for **2**$^{\bullet+}$ and a quarter that of

(10) Nelsen, S. F.; Weisman, G. R.; Hintz, P. J.; Olp, D.; Fahey, M. R. *J. Am. Chem. Soc.* **1974**, *96*, 2916.

(11) Nelsen, S. F.; Cunkle, G. T.; Evans, D. H.; Haller, K. J.; Kaftory, M.; Kirste, B.; Kurreck, H.; Clark, T. *J. Am. Chem. Soc.* **1985**, *107*, 3829.

(12) (a) Bauld, N. L.; Farr, F. R. *J. Am. Chem. Soc.* **1974**, *96*, 5633, 5634. (b) Cessac, J.; Bauld, N. L. *Ibid.* **1976**, *98*, 2712.

Table III. Parameters for Variable-Temperature ESR Simulation of **4**-d_{12}

temp, °C	a(2N), G	line width, G	k, $s^{-1} \times 10^7$
$-25._9$	20.93	0.85	44.9
$-34._4$	20.95	0.85	28.2
$-59._7$	20.96	0.75	10.6
$-76._6$	21.03	0.85	3.52
$-83._9$	21.04	0.75	2.38
$-90._9$	21.05	0.85	1.23
$-100._5$	21.06	1.0	0.616
$-106._4$	21.08	1.1	0.264

the −7 mG/deg observed for $\mathbf{21}^{\bullet+}$, which has a(2N) of 17.9_6 G at −82 °C.[10] The slope of the a(2N) vs. T curve should depend upon the shape of the potential energy, nitrogen atom bending curve on both sides of the equilibrium structure. A simple relationship between either the amount of bend at equilibrium or the double nitrogen inversion barrier and the temperature coefficient of the nitrogen splitting is neither expected nor found experimentally. The ESR spectrum of $\mathbf{4}^{\bullet+}$ clearly showed alternating line width phenomena[13] as the temperature was lowered, but there was not enough resolution to enable us to extract reliable splitting constants and allow measurement of the barrier to double nitrogen inversion. Because we expected the largest splittings to be shown by the exo hydrogens in the two carbon bridges, we replaced all of the other hydrogens by deuterium, by adding cyclopentadiene-d_6 to **5**-d_6 and reducing with unlabeled diimide, which gave the desired **4**-d_{12}. As we had hoped, the other splittings were small enough that their a(D) values of 15% the size of a(H) led to observed line narrowing, despite the complications of a substantial

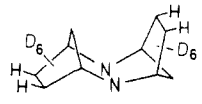

4-d_{12}

increase in the theoretical number of lines (I(D) = 1, I(H) = $^1/_2$). We were able to simulate the lowest temperature spectra taken, which were well below the apparent temperature of maximum broadening of about −85 °C, using a(2H) = 6.85, a(2H) = 1.40 G, and a line width of 1.1 G. Simulation of the spectra at various temperatures with the dynamic ESR program of Heinzer[14] and the above proton splittings gave the rate constants of Table III, for which an Eyring plot is shown in Figure 3. These data give $\Delta H^{\ddagger}$ = 4.65 kcal/mol, $\Delta S^{\ddagger}$ = 0.4 cal/(deg·mol), so $\Delta G^{\ddagger}$(−85 °C) is 4.6 kcal/mol. The only double nitrogen inversion barrier for a hydrazine cation radical previously reported is a far less accurate estimate of 3.4 kcal/mol at −110 °C from a single temperature measurement on $\mathbf{21}^{\bullet+}$.[10] This work shows that $\mathbf{4}^{\bullet+}$ is pyramidal enough at nitrogen that it has a double nitrogen inversion barrier about 17% that of neutral **4**. No conformationally caused line broadening was observed for $\mathbf{2}^{\bullet+}$, which must have a substantially lower inversion barrier.

Calculated Geometries and Inversion Barriers of Sesquibicyclic Hydrazines and Their Cation Radicals. The experimental data discussed above provide exacting experimental tests for the effects of restricting the CNN angles in sesquibicyclic hydrazines, and we consider here how well calculations are able to rationalize the experimental data. It is still not possible for us to do geometry-optimized ab initio calculations at a high enough level to have any hope for obtaining accurate results on molecules as large as those considered here. It has been pointed out that even 6-31G* level calculations on the UV λ(m) of $H_4N_2^+$ are in serious error but that semiempirical MNDO level calculations do a surprisingly good job.[15] Although the MNDO method successfully reproduces a large geometry change at nitrogen upon electron removal from

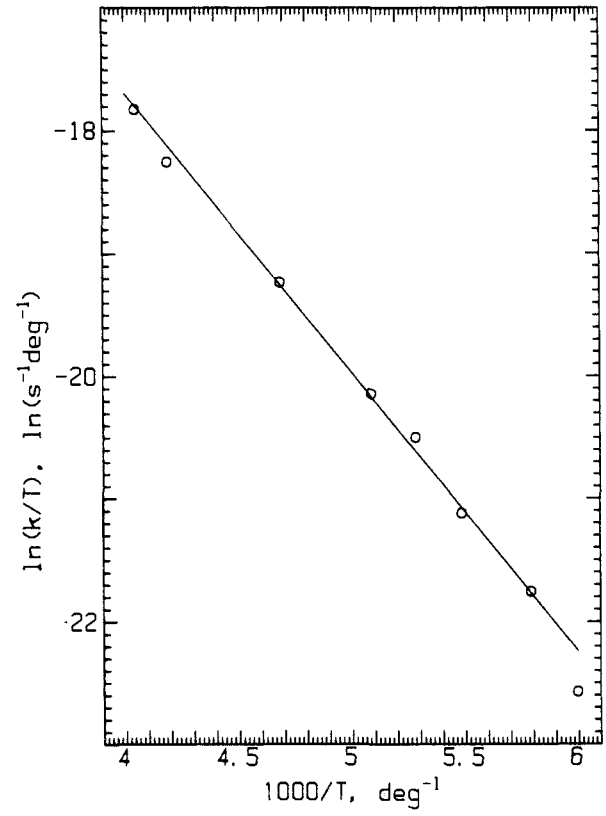

Figure 3. Eyring plot of the data of Table III.

1 and **2**, the NN bond lengths obtained are too short and the amount of flattening at nitrogen too great, compared to the experimental X-ray crystallographic structures.[3] Furthermore, MNDO calculations do not indicate the trends properly at all when the CNN angle is restricted, because $\mathbf{4}^{+}$ is calculated to still be nearly planar (α(av) = 119.6, Ψ = 10°), and the double nitrogen inversion barrier is calculated to be only 0.2 kcal/mol, in direct contradiction to experiment. Thus although MNDO calculations are quite useful for certain purposes, they do not give good enough structures for reasonable estimations of structural effects on nitrogen inversion barriers.

In this work, we have examined the use of Dewar's newer AM1 method.[16] The AM1 Hamiltonian was designed to correct the nonbonded interactions which are clearly overemphasized in earlier methods, and its use greatly improves the results for alkylated amino nitrogen compounds. Although AM1 still does not correctly predict the nearly perpendicular lone pairs of hydrazine itself,[16] it does give a minimum energy structure for tetramethylhydrazine which has θ about 82° and is thus a great improvement over MNDO, which gets the rotational curve for tetramethylhydrazine inverted, with gauche lone pair structures at the energy maximum, instead of having them the most stable ones. Even more encouragingly, AM1 predicts a single nitrogen inversion barrier of $\Delta H^{\ddagger}$ = 6.4 kcal/mol, which is not far from the observed inversion barrier of $\Delta G^{\ddagger}$ = 7.5 kcal/mol (Table I). The hydrazines considered here have considerably different structural constraints, but the comparison of X-ray crystallographic and calculated structural data for **1** and $\mathbf{1}^{\bullet+}$ given in Table IV shows that AM1 calculations do a rather good job on these structures. Although the NN bond length is still calculated as being substantially too short, especially for the neutral compounds, the average amount of bend at nitrogen measured by α(av) or Ψ is quite close to the X-ray values for the AM1 calculations, in contrast to the MNDO calculations. AM1 gets a double nitrogen inversion barrier for **4** of $\Delta H^{\ddagger}$ = 37.0 kcal/mol, which is substantially higher than the

(13) (a) Hudson, A.; Luckhurst, G. R. *Chem. Rev.* **1969**, *69*, 191. (b) Sullivan, P. D.; Boulton, J. R. *Adv. Magn. Reson.* **1970**, *4*, 39.

(14) Heinzer, J., Program No. 209, Quantum Chemistry Program Exchange, Bloomington, IN.

(15) Nelsen, S. F.; Blackstock, S. C.; Yumibe, N. P.; Frigo, T. B.; Carpenter, J. E.; Weinhold, F. *J. Am. Chem. Soc.* **1985**, *107*, 143.

(16) Dewar, M. J. S.; Zoebisch, E. G.; Healy, E. F.; Stewart, J. P. *J. Am. Chem. Soc.* **1985**, *107*, 3902. We thank Dr. Stewart for providing a copy of program MOPAC 2.14 and more recently, 3.00, which were used for the AM1 calculations.

Scheme I

	col. 1 ΔH_f(azo + diene), kcal/mol	col. 2 $\Delta\Delta G°(H^+)$, kcal/mol	col. 3 adduct ΔH_f range
a. 25 + → 1	53.3	12.6	51.3–61.9
b. 5 + → 28	75.0	14.1	73.0–83.1
c. 25 + → 26, 29	62.0		
d. 5 + → 24	81.7	13.3	79.7–89

Table IV. Comparison of Calculated and X-ray Crystallographic Structures of **1**, **2**, and Their Oxidized Forms

	neutral **1**			neutral **2**		
	X-ray	MNDO	AM1	X-ray	MNDO	AM1
d(NN), Å	1.497	1.406	1.417	1.492	1.396	1.410
ave d(CN), Å	1.491	1.501	1.495	1.474	1.495	1.488
α(CNN), deg	110.1	112.4	111.7	108.7	112.6	112.8
α(CNC), deg	116.2	119.6	114.6	118.6	121.6	116.0
α(av), deg	112.1	114.8	112.7	112.8	115.6	113.9
Ψ, deg	50.5	41.4	50.1	47.8	37.9	46.0
ΔH_f, kcal/mol	–	55.8	62.6	–	27.8	30.7
	cation radical $\mathbf{1}^{\bullet+}$			cation radical $\mathbf{2}^{\bullet+}$		
	X-ray	MNDO	AM1	X-ray	MNDO	AM1
d(NN), Å	1.349	1.325	1.335	1.325	1.315	1.324
av d(CN), Å	1.479	1.507	1.494	1.472	1.507	1.505
α(CNN), deg	113.7	114.1	113.7	114.4	114.7	114.3
α(CNC), deg	125.8	130.2	125.8	126.0	130.6	125.6
α(av), deg	117.7	119.5	117.8	118.3	120.0	118.1
Ψ, deg	27.4	11.8	26.8	24.1	0.0	25.0
ΔH_f, kcal/mol	–	213.2	222.2	–	179.6	181.9

	dication $\mathbf{2}^{2+}$		
	X-ray	MNDO	AM1
d(NN), Å	1.270	1.263	1.274
av d(CN), Å	1.471	1.546	1.515
α(CNN), deg	115.8	115.4	115.2
α(CNC), deg	128.5	129.0	129.5
α(av), deg	120.0	120.0	120.0
Ψ, deg	0.0	0.0	0.0
ΔH_f, kcal/mol	–	479.1	466.5

observed $\Delta H^{\ddagger}$ of 27.0 kcal/mol, so AM1 does not do a very good job at estimating the energy of planar neutral hydrazines. The key improvement in AM1 is for the cation radicals, because it successfully predicts a significant double nitrogen inversion barrier for $\mathbf{4}^{\bullet+}$, giving $\Delta H^{\ddagger}$ of 3.8 kcal/mol, to be compared with the 4.6-kcal/mol barrier measured experimentally in this work. For a comparison of the bending curves for $\mathbf{4}^{\bullet+}$ calculated by MNDO and AM1, see Figure 4. Because the amount of bend at nitrogen in hydrazines and their cation radicals is directly related to the lone-pair hybridization, we believe the ability of AM1 to calculate the amounts of bend will prove to be very useful in considering a variety of reactivity problems and will return to this theme in subsequent work.

Thermodynamics of Proton-Driven Diels–Alder Reactions. Scheme I is designed to address the question of why cyclopentadiene failed to add to **25** (reaction c), although the other three cases all proceeded in the presence of acid. The experimental heats of formation of 1,3-cyclohexadiene and cyclopentadiene are 25.4 and 32.1 kcal/mol, respectively,[16] while that of diazabicycloheptene **5** is 49.6 kcal/mol.[17] We suggest that a reasonably reliable estimate of the heat of formation of **25** at 29.9 kcal/mol can be obtained from the measured value for 1,4-dimethyl **25** of

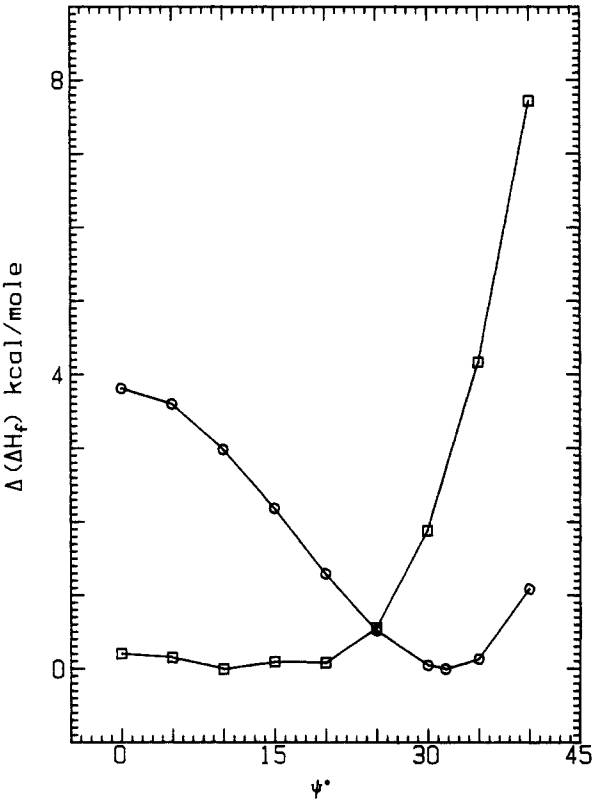

Figure 4. Comparison of energy vs. Ψ curves for bending at nitrogen of $\mathbf{4}^{\bullet+}$. Circles are calculated by AM1, squares by MNDO.

22.1 kcal/mol,[17] its AM1 calculated value of 20.3 (1.8 kcal/mol lower than experiment), and the AM1 calculated value of **25**, 28.1 kcal/mol. The sum of the heats of formation for the azo compound and diene on the left-hand side of equations a–d is given in column 1 of Scheme I. **1**, **28**, and **24** all cleave to their components without any adduct being detected at equilibrium, so eq a, b, and d are all endothermic, by an estimated 2 kcal/mol. These reactions are all exothermic when the protonated azo compound is employed, proceeding to completion by NMR. The increased driving forces upon protonation for reactions a and b have been measured in water by determining the pK_a values of protonated **1** and **25**, and **28** and **5**; the differences in pK_a converted to kcal/mol effects upon $\Delta G°$ for the addition reaction by multiplying by $2.3RT$ = 1.36 kcal/mol, appear in column 2. Although **24** cleaves too rapidly to allow its pK_a to be measured, we estimated a value from the saturated analogue **4** and the difference between related saturated and unsaturated compounds and also include the resulting $\Delta\Delta G°(H^+)$ in column 2. All of the reactions shown will have a negative $\Delta S°$ value, and although none have been measured, we expect them to be similar in size. For this discussion, we employ a $-T\Delta S°$ term of 4 kcal/mol, corrresponding to $\Delta S°$ of −13.3 eu at room temperature. The above assumptions give

(17) Engel, P. S. *J. Am. Chem. Soc.* **1976**, *98*, 1972.

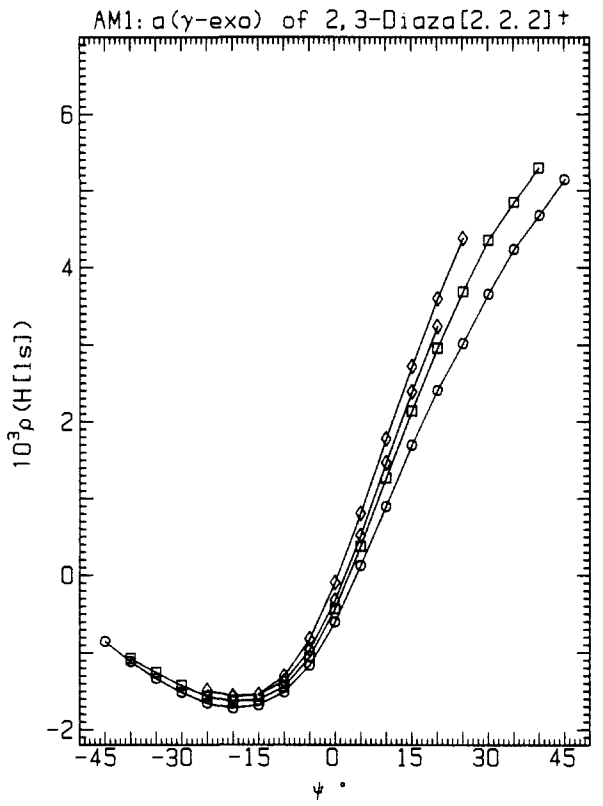

Figure 5. AM1 calculated A_γ values for 2,3-diazabicyclo[2.2.2]octane derivatives: circles, $17^{\bullet+}$; squares, $1^{\bullet+}$; diamonds, $2^{\bullet+}$.

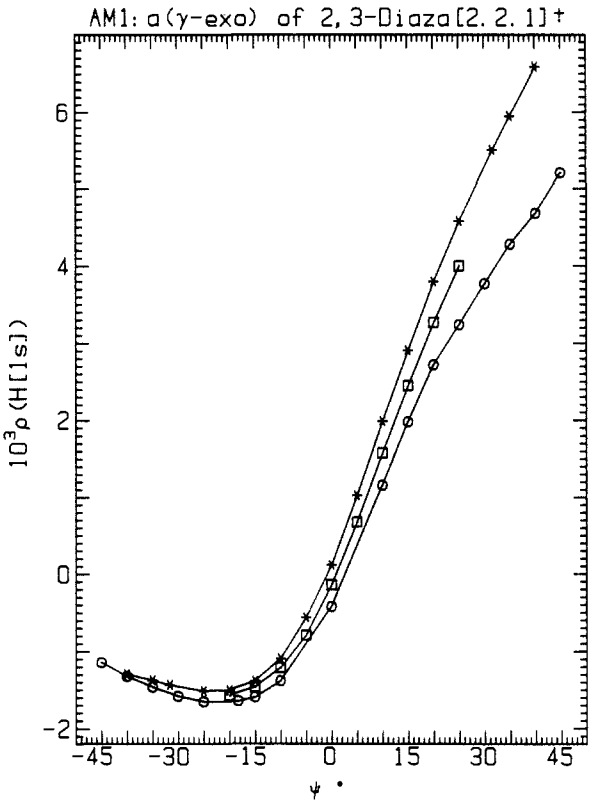

Figure 6. AM1 calculated A_γ values for 2,3-diazabicyclo[2.2.1]heptane derivatives: circles, $16^{\bullet+}$; squares, $3^{\bullet+}$; asterisks, $4^{\bullet+}$.

the ranges for adduct heats of formation shown in column 3, and while great accuracy cannot be claimed, it is clear that the reactions lying to the left in the absence of acid and to the right in its presence limit the possible ΔH_f of the adducts. Thus eq b is estimated to be not more than about 8 kcal/mol exothermic in the presence of acid. The left-hand side of eq c provides 13 kcal/mol less driving force than does that of b, and acid should be less effective at lowering the free energy because $\mathbf{25H^+}$ is about 1.8 pK units less acidic than is $\mathbf{5H^+}$. Equation c could only proceed if **26** or **29** were substantially lower in heat of formation than **28**. This is not going to be the case. These isomers differ in double bond position, and the bicycloheptenyl double bonds of **26** and **29** should lead to higher heats of formation than for the bicyclooctenyl **28** by several kcal/mol. These compounds have all been calculated by AM1, but it is clear that this method does not give reliable heats of formation for these compounds for consideration of the thermodynamics without use of corrections,[18] as among other problems, AM1 substantially overestimates the strain in bicycloheptenyl systems. We believe these considerations make it clear that the reaction of eq c fails because it is simply too endothermic even for protonation to provide enough driving force and wish we had realized this before we spent so much time trying to get the reaction to go.

Long-Range Splittings and Bending at Nitrogen. The ESR data of Table II show that the H[γ-exo] splittings of the two carbon bridges of bicyclic hydrazines are very sensitive to the direction of bending at nitrogen, and we have examined AM1 calculations to see if they will help quantitate the amount of bending present in these cations. The results of AM1 (and MNDO calculations, which give similar splittings but much more poorer equilibrium geometries) are initially very disappointing, because the observed splitting patterns are not reproduced. Substantially negative γ spin densities are calculated in many cases for hydrogens which only show small ESR splittings. ρ(H[1s]) should be directly proportional to the observed a(H) values. Pople and co-workers have used a proportionality constant of 540 for INDO calculations,[19] but a larger value appears to be necessary for AM1 calculations, and 1000 appears to be about right for methyl splittings of hydrazine cations (to be discussed elsewhere) and we shall use $10^3\rho$(H[1s]) values as "calculated splittings" here. Plots of calculated a(H[γ-exo]) values (which we will refer to as A_γ for brevity) for the two carbon bridges in the compounds under consideration here are shown in Figures 5 and 6. They show that the calculations do reproduce the experimentally required substantial increase in A_γ when the direction of bend at nitrogen enforces back lobe overlap (see "W-plan"[22] below) over that for bend in the opposite sense (see "non-W"). The shape of the

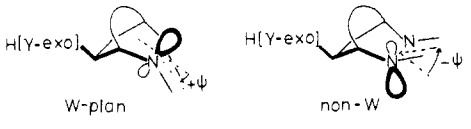

calculated curves is very similar for the [2.2.2] and [2.2.1] systems, with slightly more positive calculated A_γ values occurring when the alkyl substituents are linked to constrict the NNC angles to lower values. The calculated negative A_γ values for negative Ψ

(18) By AM1: ΔH_f(5) = 62.6 kcal/mol (13.0 higher than experiment), $\Delta H_f(C_5H_6)$ = 37.1 (5.0 higher than experiment), $\Delta H_f(C_6H_8)$ = 17.3 (8.3 lower than experiment), ΔH_f(**1**) = 62.6, ΔH_f(**28**) = 87.2, ΔH_f(**26**) = 97.4, ΔH_f(**29**) = 97.0, ΔH_f(**24**) = 124.4 kcal/mol.

(19) Pople, J. A.; Beveridge, D. L.; Dobosh, P. A. *J. Am. Chem. Soc.* **1968**, *90*, 4201.
(20) King, F. W. *Chem. Rev.* **1976**, *76*, 157.
(21) Nelsen, S. F.; Teasley, M. F.; Bloodworth, A. J.; Eggelte, H. J. *J. Org. Chem.* **1985**, *50*, 3299.
(22) The utility of NCG approximations was pointed out to us by Timothy Clark (Erlangen).

values certainly are incorrect, however. Symmetrical bicyclo[2.2.2]octyl systems would have to exhibit much lower A_γ values than they do if this were the case, and the equilibrating and frozen spectra of **4**-d_{12}^+ demonstrate that both signs for Ψ have the same sign for A_γ. The calculated $10^3\rho$(H[γ-exo]) values at the energy minimum for $\mathbf{4}^{\bullet+}$ are 5.56 and −1.43, 1.29 and 2.83 negative of the observed A_γ values at low temperature. It is also clear experimentally that A_γ should be significantly positive at $\Psi = 0°$. For 2,3-dioxybicyclooctane cation radical, which has $\Psi = 0°$ by default because there are no substituents external to the bicyclic ring to bend out of plane, AM1 obtains $10^3\rho$(H[γ-exo]) of only +0.37, while the experimental A_γ is 4.70 G.[23] The problem of getting far too negative calculated γ splittings for non-aligned γ-hydrogens is quite general for AM1 (and MNDO), as shown by the calculated values for the endo two carbon bridge and both one carbon bridge protons in bicyclo[2.2.1]heptyl systems, which will not be documented in detail here.

One prediction we made when we started this work turned out to be completely untrue. We expected that nonbonded interactions between the syn two carbon bridges of **2** would force its cation to be unusually flat for a tetraalkylhydrazine cation radical. The X-ray structure of $\mathbf{2}^{\bullet+}$ showed that it is far from flat at nitrogen, and AM1 calculations give an equilibrium structure with Ψ = 25.0°, close to the 24.1° obtained by X-ray. The A_γ splitting of $\mathbf{2}^{\bullet+}$ of 2.87 G is larger than that of the dimethyl compound $\mathbf{17}^{\bullet+}$, 2.46 G, indicating that the sesquibicyclic system is not even as flat as the dimethyl compound in solution, and the AM1 equilibrium structure for $\mathbf{17}^{\bullet+}$ is also flatter, at $\Psi = 17.8°$. $\mathbf{4}^{\bullet+}$ is obviously more pyramidal at nitrogen than its dimethyl analogue $\mathbf{16}^{\bullet+}$, but it has a smaller A_γ splitting, 4.2 vs. 4.8 G, which initially seems anomalous. AM1 calculations indicate a reasonable explanation; the minimum energy structure is calculated to have endo-bent methyl groups, $\Psi = 21.8$, the exo-bent energy minimum occurring at $\Psi = -18.6$, and lying a calculated 0.15 kcal/mol higher in energy. The larger A_γ endo bent conformations should predominate for $\mathbf{16}^{\bullet+}$, but they are equal in energy for $\mathbf{4}^{\bullet+}$. Unfortunately, AM1 does such a poor job at getting the magnitude of the A_γ splittings at small positive and negative Ψ values that it seems unfruitful to try to see if the bending curves calculated by AM1 are reasonably correct by calculating the A_γ splittings with averaging between the conformations. We hope to address this question by examining the nitrogen splittings for a range of tetraalkylhydrazine cations in a separate paper.

UV Spectra of Sesquibicyclic Cation Radicals. Another spectral property of hydrazine cation radicals which is sensitive to pyramidalization at nitrogen is the optical absorption maximum. Promotion of an electron from the doubly occupied π to the singly occupied π^* orbital of the lone-pair π system causes absorption in the near-ultra-violet (UV) region for most tetraalkylhydrazine cation radicals, but the absorption maximum, λ(m), proves to be very sensitive to the structure of the alkyl groups, in contrast to most UV absorptions. There can be no mixing of the lone-pair π orbitals with σ(NN) and σ(CN) orbitals when the nitrogen atoms are planar, but such σ,π mixing becomes increasingly important as the nitrogens bend. Furthermore, bending syn at the nitrogens, as occurs for sesquibicyclic compounds, causes substantially larger mixing than bending anti, because of symmetry effects; a high-lying σ orbital has the proper symmetry to mix with the nitrogen-centered π orbital for syn-bent systems but can only mix with nitrogen-centered π^* in anti-bent compounds.[15] This difference in orbital symmetry is reflected in larger red shift of λ(m) and larger ESR a(N) values for syn-bent hydrazines than for anti-bent ones of similar amount of pyramidalization at nitrogen. Qualitative comparisons of experiment with calculations were made with the "neutral in cation geometry" (NCG) approximation,[15,22] in which it was pointed out that energy gaps corresponding to the π,π^* transitions were well approximated from the energy separations between the π and π^* orbitals in an MO calculation of the neutral compound which is held in the geometry of the cation radical. Thus Koopman's theorem works well when the occupancy of the orbitals involved is the same; obviously, this NCG approximation method will not work for non-Koopmans transitions.[23]

Table V. UV Absorptions for Sesqubicyclic Hydrazine Cation Radicals in Acetonitrile

cation	anion	λ(m), nm (ϵ, M^{-1} cm^{-1})
$\mathbf{1}^+$	NO_3^-	286 (1400), 272 (1500)
$\mathbf{1}^+$	PF_6^-	286 (1400), 272 (1500), 221 (1900)
$\mathbf{2}^+$	NO_3^-	266 (1600), 204 (9600)
$\mathbf{2}^+$	PF_6^-	266 (1800), 244 (1700), 218 (1800)
$\mathbf{2}^+$	BF_4^-	264 (1600), 243 (1500)
$\mathbf{28}^+$	NO_3^-	sh 304, 280 (1200)
$\mathbf{3}^+$	NO_3^-	283 (1800)
$\mathbf{4}^+$	NO_3^-	321 (700)

Table V summarizes UV data for sesquibicyclic hydrazine radical cations. An absorption of about 220 nm is observed for the PF_6^- salts of both $\mathbf{1}^+$ and $\mathbf{2}^+$, but not for their NO_3^- or BF_4^- salts. We presume that this transition involves charge transfer between the ions.

Two UV maxima are shown for $\mathbf{1}^+$, $\mathbf{2}^+$, and $\mathbf{28}^+$, although they are close enough together that they overlap badly. In previous work we had assumed that the longest wavelength band is the π,π^* absorption, which was consistent with NCG MO calculations, but we shall now consider the origin of the second band in the near UV of some of the compounds of Table V. These systems share the presence of 2,3-diazabicyclo[2.2.2]octyl part-structures. Hoffmann and co-workers[24] pointed out that the highest lying cyclohexane orbitals have AA and SS symmetry with respect to the planes shown below and discussed the importance of symmetry considerations in σ,π mixing in norbornyl systems containing a

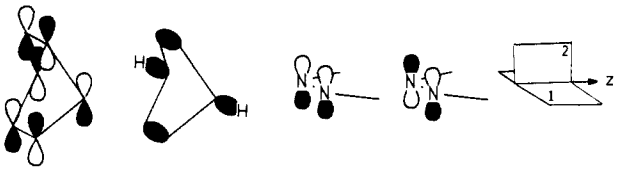

σ (AA) σ (SS) π (AS) π*(AA)

p orbital centered at position 7 in terms of interacting the cyclohexane orbitals with the p orbital. The compounds under discussion have the NN system π and π^* which may be considered to interact in a similar manner. π^*(AA) and σ(AA) will mix, giving symmetric and antisymmetric combination orbitals. The UV transition between the doubly occupied σ(AA)[$+\pi^*$(AA)] and the singly occupied π^*(AA)[$-\sigma$(AA)] is allowed (in the z direction, in which the doubly occupied orbital is bonding, and the singly occupied orbital antibonding). MNDO calculations

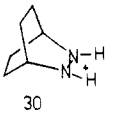

30

by the NCG method on model system **30** with the nitrogens planar do predict two transitions of similar energy, λ(m) = 280 nm for the π(AS),π^*(AA) transition and 264 nm for the σ(AA),π^*(AA) transition, with relative intensities approximated by Mulliken's dipole moment vector method neglecting differential overlap[25] of 4:1.

We shall not consider the correlation of λ(m) and a(N) in detail here. AM1 calculations give rather longer wavelength λ(m) values than do MNDO calculations when used in the NCG approximation. The problem of averaging the bending at nitrogen over the occupied conformational ranges, which we believe to be very different for different tetraalkylhydrazines, and also should be

(23) Shida, T.; Haselback, E.; Bally, T. *Acc. Chem. Res.* **1984**, *17*, 180.

(24) Hoffmann, R.; Mollere, P. D.; Heilbronner, E. *J. Am. Chem. Soc.* **1973**, *95*, 4860.

(25) (a) Mulliken, R. S. *J. Chem. Phys.* **1939**, *7*, 14. (b) Jaffe, H. H.; Orchin, M. *Theory and Applications of Ultraviolet Spectroscopy*; Wiley: New York, 1962; Chapter 6. (c) Jaffe, H. H.; Orchin, M. *Symmetry, Orbitals, and Spectra*; Wiley-Interscience: New York, 1971; Chapter 8.

very different for ESR and optical experiments because of their very different time scales, will have to be examined in detail to make significant progress in understanding such a correlation.[15]

Experimental Section

2,7-Diazatetracyclo[6.2.2.1^{3,6}.0^{2,7}]tridecane Radical Cation Nitrate ($3^+NO_3^-$). Neutral **3** (28 mg, 0.157 mmol) in 1 mL of CH_3CN was cooled to 0 ± 5 °C. One equivalent of $AgNO_3$ (26 mg) in 1 mL of CH_3CN was added and a gray precipitate formed immediately (Ag°). After 30–60 min at 0 °C with occasional mixing, the mixture was filtered through a glass wool plug. Ether was added to precipitate a white powdery solid, and the solvent was removed via canula. After two more washings with ether and removal of residual solvent in vacuo there remained a white solid, 33.7 mg (0.140 mmol, 89%). Anal.[26] Calcd for $C_{11}H_{18}N_3O_3$: C, 54.98; H, 7.55; N, 17.48. Found: C, 53.27; H, 7.16; N, 16.89. This analysis would be within acceptable limits if 3.1% of the sample did not contain CHN; silver is the most likely contaminant.

2,7-Diazatetracyclo[6.2.1.1^{3,6}.0^{2,7}]dodecane Radical Cation Nitrate ($4^+NO_3^-$). Neutral **4** (32.4 mg, 0.2 mmol) in 1 mL of CH_3CN was cooled to −20 ± 10 °C. One equivalent of $AgNO_3$ (34 mg) in 1 mL of CH_3CN was added, a grey precipitate immediately formed, and the solution turned yellow. After 30–60 min at cold temperatures with continued stirring, the mixture was filtered through a glass wool plug under nitrogen. Ether was added to precipitate out a light yellow solid, and solvents were removed via canula. After two more washings, with ether and removal of residual solvent in vacuo there was obtained 32 mg of a light yellow powdered solid (0.143 mmol, 72%). Anal.[26] Calcd for $C_{10}H_{16}N_3O_3$: C, 53.09; H, 7.13; N, 18.57. Found: C, 51.97; H, 6.92; N, 18.13. This analysis would be within acceptable limits if 2.1% of the sample did not contain CHN; silver is the most likely contaminant.

2,7-Diazatetracyclo[6.2.2.1^{3,6}.0^{2,7}]tridec-9-ene Radical Cation Nitrate ($28^+NO_3^-$). Neutral hydrazine **28** (87.4 mg, 0.50 mmol) in 2 mL of CH_3CN was cooled to −20 °C under nitrogen. To this was added via canula 1 equiv of $AgNO_3$ (84.4 mg) in 1 mL of CH_3CN cooled to −20 °C. A grey precipitate forms, and the solution turned a deep yellow color. The mixture was kept at −20 ± 10 °C for 60 min, with occasional mixing. The solution was then filtered to remove the silver through a glass wool plug into a flask at −20 °C under nitrogen. Ether was added to precipitate out the radical cation salt as a dark yellow solid, and solvent was removed via canula. The product was washed twice more with ether, and residual solvent was removed in vacuo to give 108.9 mg of a dark yellow powder (0.46 mmol, 92%). Anal.[26] Calcd for $C_{11}H_{16}N_3O_3$: C, 55.45; H, 6.77; N, 17.64. Found: C, 54.30; H, 6.66; N, 17.29. This analysis would be within acceptable limits if 2.1% of the sample did not contain CHN; silver is the most likely contaminant.

***exo,exo*-5,6-Diprotio-2,3-diazabicyclo[2.2.1]hept-2-ene-d_6 (5-d_6).** Perdeuteriocyclopentadiene was obtained follwing a procedure of Solomon.[27] Percent deuterium incorporation was estimated with use of ^1H NMR analysis of a Diels–Alder adduct of the perdeuteriocyclopentadiene and maleic anhydride (>95%). The d_6 cyclopentadiene was used directly in the synthesis of 5-d_6 following a preparation by Roth[28] for the synthesis of the *exo,exo*-5,6-d_2-**5**, with appropriate substitution of cyclopentadiene in the initial addition and deuterium in the hydrogenation. The final product was purified by sublimination. ^1H NMR ($CDCl_3$): δ 1.49 (s).

1,8,11,11-*endo*,*endo*-9,10-hexadeuterio-2,7-diazatetracyclo-[6.2.1.1^{3,6}.0^{2,7}]dodecane (4-d_6). To 70 mg (0.687 mmol) of 5-d_6 in 3 mL of CH_3CN was added 1 equiv of HBF_4·Et_2O (82.5 μL) with stirring. To this solution was added 2 equiv of cyclopentadiene (100 μL), freshly cracked and dried over $CaCl_2$. After 15 min of stirring, this solution was added to a stirring mixture of 0.9 g of KO_2C—N=N—CO_2K (10 equiv) in 10 mL of CH_3CN at 0 °C. Next, 2 mL of glacial acetic acid were added slowly to avoid vigorous foaming. After 1 h at 0 °C, the mixture was gradually warmed to room temperature and then stirred overnight. For workup, the mixture was passed through a fine fritted glass filter and the volatiles were removed by rotoevaporater. Et_2O (15 mL) was added, the mixture was cooled to 0 °C, and 2 g of crushed NaOH were then added. This mixture was rapidly filtered under nitrogen through a fine glass frit, and the ether is distilled off at 0 °C under reduced pressure. Residual solvent was removed in vacuo, and this crude material used as described in the VT–NMR experiments. ^1H NMR (CD_3CN) δ 3.37 (br s, 2 H), 1.93 (br d, 1 H, J = 11 Hz), 1.77 (m, 2 H), 1.15–1.42 (m, 5 H). High-resolution MS, parent ion m/e calcd for $C_{10}H_{10}D_6N_2$ 170.1688, found 170.1692 (m/e 170, 27.49% intensity of base peak 66).

Tetra-*exo*-4,5,9,10-tetraprotio-2,7-diazatetracyclo[6.2.1.1^{3,6}.0^{2,7}]dodecane-d_{12} (4-d_{12}). The procedure used here followed that used for 4-d_6 above except that in the initial Diels–Alder addition to 94 mg (0.93 mmol) of 5-d_6H^+, 2 equiv of cyclopentadiene-d_6 were used instead of cyclopentadiene. The crude product was Kugelrohr distilled to give 37 mg of product (0.21 mmol, 23%). ^1H NMR ($CDCl_3$) δ 1.49 (s, 2 H), 1.36 (s, 2 H). High-resolution MS, parent ion m/e calcd for $C_{10}H_4N_2D_{12}$ 176.2066, found 176.2059 (m/e 176, 17.70% intensity of base beak 72).

Variable-temperature ^{13}C NMR work on **2** was as described previously (Table I, footnote *c*). VT ^1H NMR work on 4-d_6 was performed with an IBM Brucker 200 MHz FT–NMR equipped with a variable-temperature probe and a Brucker B-ST 100/700 Variable Temperature controller. Temperatures were recorded on a Doris Model 400A Trendicator thermocouple lowered inside the probe previous to each run. In a typical experiment, a 10-mg sample of 4-d_6 was taken up in 1 mL of Me_2SO-d_6, passed through a plug of basic alumina, and transferred under nitrogen to a 5-mm NMR tube. *tert*-Butylbenzene (0.5 mol equiv, Aldrich, 99%) was added for reference. For the experiment at 91.9 °C, spectra were recorded every 2 to 3 min for about 1 h, at which time the bridgehead signal at δ 3.37 had nearly fully grown in. Lower temperatures required longer observation times.

ESR spectra were recorded on a Varian E.15 system. $27^{\bullet+}$, $17^{\bullet+}$, $15^{\bullet+}$, and $16^{\bullet+}$ samples were prepared by oxidation with aminium cation radicals.[10] Isolated $1^{\bullet+}$ and $2^{\bullet+}$ were dissolved in deoxygenated CH_3CN. For compounds **3**, **4**, **28**, and 4-d_{12}, the radical cation was generated in solution by adding I equiv of $AgNO_3$ to a deoxygenated solution of the neutral. UV spectra were recorded on a Cary 118 instrument; isolated radical cation salts of **1**, **2**, **3**, **4**, and **28** were simply dissolved in CH_3CN.[15]

Acknowledgment. We thank the National Science Foundation and the National Institutes of Health for partial financial support of this work under grants CHE-8415077 and GM-29549. We thank Gary Wesenberg for help in implementing the dynamic ESR program on the Harris 7 computer.

(26) Spang Microanalytical Laboratory, Eagle Harbor, MI.
(27) Salomon, R. G.; Zagorski, M. G. *J. Am. Chem. Soc.* **1982**, *104*, 3498.
(28) Roth, R. W. *Annalen* **1967**, *702*, 1.